Fermi National Accelerator Laboratory

FERMILAB-Pub-76/36-EXP
7100.186

ANALYSIS OF DIFFRACTIVE pd → Xd AND pp → Xp INTERACTIONS AND TEST OF THE FINITE MASS SUM RULE

Y. Akimov, L. Golovanov, S. Mukhin, and V. Tsarev
Joint Institute for Nuclear Research, Dubna, USSR

and

E. Malamud, R. Yamada, and P. Zimmerman
Fermi National Accelerator Laboratory, Batavia, Illinois 60510 USA

and

R. Cool, K. Goulianos, and H. Sticker
Rockefeller University, New York, New York 10021 USA

and

D. Gross, A. Melissinos, D. Nitz, and S. Olsen
University of Rochester, Rochester, New York 14627 USA

April 1976

Operated by Universities Research Association Inc. under contract with the Energy Research and Development Administration

FERMILAB-Pub-76/36-EXP

Rockefeller University
COO-2232A-31

University of Rochester
UR-572

ANALYSIS OF DIFFRACTIVE $pd \to Xd$ and $pp \to Xp$ INTERACTIONS AND TEST OF THE FINITE MASS SUM RULE[*]

Y. Akimov, L. Golovanov, S. Mukhin,
v, L. Golovanov, S. Mukhin, G. Takht and V. Tsarev[†]
Joint Institute for Nuclear Research, Dubna, USSR

E. Malamud, R. Yamada, and P. Zimmerman[‡]
Fermi National Accelerator Laboratory, Batavia, Illinois 60510 USA

R. Cool, K. Goulianos, and H. Sticker
Rockefeller University, New York, New York 10021 USA

and

D. Gross, A. Melissinos, D. Nitz, and S. Olsen[§]
University of Rochester, Rochester, New York 14627 USA

Cross-sections for the reaction $pp \to Xp$ in the diffraction dissociation region, extracted from the recently reported precise Fermilab data on $pd \to Xd$, are compared with results from Fermilab and ISR. The M_X^2, t, and s dependence are discussed and the first-moment finite mass sum rule is tested.

---

[*] Work supported in part by the U. S. Energy Research and Development Administration under Contracts No. E(11-1)-2232A and No. E(11-1)-3605, and by the U.S.S.R. State Committee for Atomic Energy.

[†] Present address: P. N. Lebedev Institute, Moscow, U. S. S. R.

[‡] Present address: Louisiana State University, Baton Rouge, La. 70803.

[§] Alfred P. Sloan Foundation Fellow.

Recently, a precise measurement of the inclusive inelastic process

$$p + d \rightarrow X + d \qquad (1)$$

in the region $50 < p_{lab} \lesssim 400$ GeV/c, $0.03 < |t| \lesssim 0.12$ (GeV/c)^2, and 1.4 GeV^2 $< M_x^{\,2} \lesssim 0.11\, p_{lab}$ was reported[1,2] . This range of $M_x^{\,2}$ includes the resonance region as well as the triple-Regge region[3] (TR region: $M_x^{\,2} >> m_p^{\,2}$ and $M_x^{\,2}/s \leq 0.1$). In this report, we analyze the pd results and we test the first-moment finite mass sum rule[4] (FMSR).

Our analysis is performed on pp → Xp cross-sections extracted from the pd → Xd data using factorization. By comparing the extracted pp → Xp results with existing data we show that factorization holds to a good approximation. In any case, since the reduction to pp → Xp cross-sections involves division by a function of t only, our conclusions about the s and $M_x^{\,2}$ dependence of the differential cross-sections and about the validity of the FMSR are very insensitive to uncertainties in the extraction procedure.

I. Factorization and Extraction of pp → Xp Cross-Sections -

The pd → Xd measurement was performed at Fermilab using an internal deuterium gas jet target. Elastic pd scattering was also studied[5] in the same p_{lab} and t-range. The elastic cross-section factorizes approximately like $(d\sigma/dt)^{pd} \simeq (d\sigma/dt)^{pp} \cdot F_d(p_{lab},t)$, where $F_d(p_{lab},t)$ is the coherence factor defined as

$$F_d(p_{lab},t) = \left[\frac{\sigma_T^{\,pd}}{\sigma_T^{\,pp}}\,(p_{lab})\right]^2 \cdot |S(t)|^2 \qquad (2)$$

Here, $\sigma_T^{pd(pp)}$ is the pd(pp) total cross-section and S(t) is the deuteron form factor. In the region of small $|t|$, the data are reasonably well described by

$$|S(t)|^2 = e^{b_0 t + ct^2} \tag{3}$$

with[5] $b_0 = 26.4 \pm 0.2\ (\mathrm{GeV/c})^{-2}$ and $c = 62.3 \pm 1.1\ (\mathrm{GeV/c})^{-4}$. Over the p_{lab} range of the pd experiment, the factor $(\sigma_T^{pd}/\sigma_T^{pp})^2$ is approximately constant and has the value[6] of 3.6 to within better than 2% accuracy. Thus, the coherence factor takes the form

$$F_d(t) \equiv F_d\ (50 < p_{lab} < 400,\ |t| < 0.12) \simeq 3.6\ e^{26.4\ t\ +\ 62.3\ t^2} \tag{4}$$

Assuming that the inelastic cross-section factorizes in the same way as the elastic,

$$\frac{d^2\sigma}{dtdM_x^{\ 2}}\ (pd \to Xd) = \left[\frac{d^2\sigma}{dtdM_x^{\ 2}}\ (pp \to Xp)\right] \cdot F_d(t) \tag{5}$$

one may then obtain cross-sections for the reaction

$$p + p \to X + p \tag{6}$$

by dividing the measured cross sections for $pd \to Xd$ by the elastic coherence factor. If the Glauber-type corrections for inelastic scattering are comparable to the corrections for elastic scattering ($\lesssim 10\%$), this procedure is expected to yield the correct cross-sections for $pp \to Xp$, including the values of the slope parameter, to within better than $\sim 10\%$.

Factorization was successfully tested[1] in the $M_x^2 < 4\ \mathrm{GeV}^2$ region for $|t| = 0.025\ (\mathrm{GeV/c})^2$ and $p_{lab} = 180$ and 275 GeV/c. In Fig. 1, we compare the extracted $pp \to Xp$ cross-sections for $p_{lab} = 275$ GeV/c and $|t| = 0.025\ (\mathrm{GeV/c})^2$ with data from Fermilab[7,8] and ISR[9], where the points of references 8 and 9 have been obtained from the measured cross-sections at $|t| = 0.15$ and 0.16, respectively, by extrapolation using a slope of $6\ (\mathrm{GeV/c})^{-2}$. The agreement at low as well as high values of M_x^2 is good within the experimental error of $\sim \pm 10\%$. The peaking of the cross-section at low M_x^2/s is striking and the $1/M_x^2$ behavior in the region $5\ \mathrm{GeV}^2 \lesssim M_x^2 \lesssim 0.05\ s$ is apparent.

II. M_x^2, t, and s Dependence of Extracted $pp \to Xp$ Cross-Sections -

In the resonance region, $M_x^2 < 5\ \mathrm{GeV}^2$, the M_x^2 distributions of the extracted pp cross-sections exhibit structure[1], with a prominent broad enhancement centered at $M_x^2 \simeq 1.9\ \mathrm{GeV}^2$ and a smaller peak at $M_x^2 \simeq 2.8\ \mathrm{GeV}^2$ probably to be identified with the $N^*(1688)$ state. A still smaller bump may be present at $M_x^2 \simeq 3.7\ \mathrm{GeV}^2$. For $M_x^2 > 5\ \mathrm{GeV}^2$, the cross-sections at fixed s behave[2] as $1/M_x^2$. The t-distributions for fixed M_x^2 are exponential[1,2] (see Fig. 2) with no sign of a turnover down to values of $|t| \simeq 0.03\ (\mathrm{GeV/c})^2$. The slope parameter, $b(M_x^2)$, seems to be a function only of M_x^2 independent of p_{lab}. In the resonance region, $b(M_x^2)$ falls very rapidly from the value of $\sim 20\ (\mathrm{GeV/c})^{-2}$ at $M_x^2 \sim 1.9\ \mathrm{GeV}^2$ to the average value[2] of $6.5 \pm 0.3\ (\mathrm{GeV/c})^{-2}$ for $M_x^2 \gtrsim 5\ \mathrm{GeV}^2$.

Fig. 3a shows $b(M_x^2)$ versus M_x^2 for $p_{lab} = 275$ GeV/c. Fig. 3b shows the differential cross-section at $t = 0$ multiplied by M_x^2, obtained by extrapolating the data at higher $|t|$-values[1,2] using the slopes in Fig. 3a. The M_x^2

distributions of $b(M_X{}^2)$ and of $M_X{}^2(d^2\sigma/dtdM_X{}^2)_{t=0}$ have a very similar shape. Dividing the values of $M_X{}^2(d\sigma/dtdM_X{}^2)_{t=0}$ in Fig. 3b by the values of the slopes in Fig. 3a yields $M_X{}^2$ times the integral over t of the differential cross-section, $M_X{}^2(d\sigma/dM_X{}^2)$, shown in Fig. 3c. Within the errors, $M_X{}^2(d\sigma/dM_X{}^2)$ is approximately constant all the way down to $M_X{}^2 \sim 1.7$ GeV^2, where it starts dropping towards the pion threshold at $M_X{}^2 \simeq 1.15$ GeV^2. Thus, the prominent low-mass enhancement at $M_X{}^2 \sim 1.9$ GeV^2 observed at small fixed t-values appears to be a manifestation of the increased value of the slope parameter. The cross-section for the production of a mass, $d\sigma/dM_X{}^2$, follows the simple $1/M_X{}^2$ behavior for all masses within the range of the pd experiment including the resonance region.

The extracted $pp \to Xp$ cross-sections in the high mass region show a non-negligible energy dependence. An adequate fit of the differential cross-section in this region is given by[2]

$$\frac{d^2\sigma}{dtdM_X{}^2} = \frac{A(1 + B/p_{lab})}{M_X{}^2}\, b_0\, e^{b_0 t} \tag{7}$$

where $A = 0.54 \pm 0.02$ mb, $B = 54 \pm 16$ GeV/c, and $b_0 = 6.5 \pm 0.3$ (GeV/c)$^{-2}$, where the uncertainties include a $\pm 3\%$ normalization uncertainty. It is remarkable that this formula also describes well the average behavior of the cross-section in the resonance region provided b_0 is replaced by $b(M_X{}^2)$ of Fig. 3a.

In the kinematic region of the data, the inclusive cross-section is expected to be described theoretically by the triple Regge formula[3]

$$\frac{d^2\sigma}{dtd\nu} = \frac{1}{s^2} \sum_{ijk} G_{ijk}(t) \left(\frac{s}{\nu}\right)^{\alpha_i(t) + \alpha_j(t)} (\nu)^{\alpha_k(0)} \tag{8}$$

where $\nu = M_x^{\,2} - m_p^{\,2} - t$ is the crossing symmetric variable, the $G_{ijk}(t)$ are the triple Regge couplings, and the $\alpha_i(t)$ are the Regge trajectories. Because the isospin of the deuteron is zero, only zero isospin i and j trajectories can contribute to the triple Regge expansion for reaction (1), excluding, for example, $\pi\pi R$ and $\pi\pi P$ couplings, which appear to contribute non-negligibly to $pp \to Xp$.

Ignoring for the moment the energy dependence of the data, the fitted result (7) shows that at each energy the ν dependence is compatible with a pure triple Pomeron coupling, for which equation (8) simplifies to

$$\frac{d^2\sigma}{dtd\nu} = \frac{G_{PPP}(t)}{\nu} \left(\frac{s}{\nu}\right)^{2\alpha' t} \tag{9}$$

From equations (9) and (7) we find that in the limit of $s \to \infty$ $G_{PPP}(t) = (3.3 \pm 0.16)\ e^{(4.9 \pm 0.5)t}$ where we have used[10] $\alpha' = 0.278\ (\mathrm{GeV/c})^{-2}$.

To account for the energy dependence of the data in the TR formalism, we must add one or more energy dependent terms to Eq. (9), for example an RRR term. A good fit to the data is obtained with PPP, RRR and PPR terms. The result, using $\alpha'_R = 1\ (\mathrm{GeV/c})^{-2}$ and fixing the slope at 5 $(\mathrm{GeV/c})^2$, is

$$\begin{aligned} G_{PPP}(t) &= (\ 3.20 \pm 0.36)\ e^{5t} \\ G_{RRR}(t) &= (\ \ 74 \pm 30\ )\ e^{5t} \\ G_{PPR}(t) &= (\ 1.00 \pm 0.63)\ e^{5t} \\ \chi^2 &= 34.6/28 \text{ degrees of freedom.} \end{aligned} \tag{10}$$

An equally good fit is obtained with only the PPP and RRR terms, in which case the triple Pomeron coupling is larger by 17%. However, the fit presented above is closer to satisfying the finite mass sum rule, as will be shown below.

III. Test of the FMSR -

The first-moment finite mass sum rule states that[4], at fixed t,

$$|t| \frac{d\sigma_{el}}{dt} + \int^{N} \nu \frac{d^2\sigma}{dtd\nu} \, d\nu = \int^{N} \nu \left[\frac{d^2\sigma}{dtd\nu} \right]_{TR} d\nu \tag{11}$$

where $d\sigma_{el}/dt$ is the differential elastic scattering cross-section, $[d^2\sigma/dtd\nu]_{TR}$ is the fit to the inelastic cross-section in the TR region smoothly extrapolated to $\nu = 0$, and N is any ν corresponding to an M_X^2 lying between resonances. For fixed t, $d\nu = dM_X^2$. Figure 4 shows (i) the values of $\nu d^2\sigma/dtdM_X^2$ versus M_X^2 derived from the pd data[1,2] at 275 GeV/c and $|t| = 0.035$ (GeV/c)^2, (ii) the experimental value of $|t| d\sigma_{el}/dt$ (derived from the pd data of Ref. 5) represented as a Gaussian shaped area for illustrative purposes and, (iii) the fit to the data in the high mass region of $\nu[d^2\sigma/dtdM_X^2]_{TR}$ with the simple form of eq. (9) extrapolated to $M_X^2 = m_p^2$, represented by the solid curve at the constant value of 3.1 mb$\cdot$(GeV/c)$^{-2}$. The sum of the areas under (i) and (ii), representing the left hand side of equation (11), equals the area under the solid curve representing the right hand side of equation (11), to within the 3% normalization uncertainty. Thus, with the simple parametrization (9) of the high mass data, the FMSR is satisfied to a high degree of accuracy. The validity of this rule for other t-values within the range of the pd → Xd experiment is equally good.

If one requires that the triple Regge parametrization, eq. 8, fit the high mass data[2], as well as the low mass[1] and elastic scattering data[5] via the FMSR, eq. 11, one obtains more accurate values for the TR couplings:

$$\begin{aligned} G_{PPP}(t) &= (\ 2.91 \pm 0.25)\ e^{5t} \\ G_{RRR}(t) &= (\ 122 \pm 15\ )\ e^{5t} \\ G_{PPR}(t) &= (\ 1.00 \pm 0.14)\ e^{5t} \\ \chi^2 &= 43.4/29 \text{ degrees of freedom} \end{aligned} \tag{12}$$

A number of other TR analyses of previously available $pp \to Xp$ data have been reported[3,11]. For example, the authors of Ref. 11 report values of the TR couplings which were determined by fitting the high energy, high mass data while constraining the solutions to agree with lower energy, low mass data through FMSR. Their best solution has non-zero PPP, RRR, PPR, and RRP couplings which, if reduced by about 10%, fit the high mass $pd \to Xd$ data well. The result of their solution #1 is $G_{PPP}(0) = 2.63$, $G_{RRR}(0) = 18.1$, $G_{PPR}(0) = 4.42$, and $G_{RRP}(0) = 31.6$ which should be compared to our results (10) and (12). Their value for G_{PPP} is somewhat smaller than our result, primarily because of the presence of a larger PPR term.

The tight correlation among the fitted parameters makes it difficult to extract a unique set of triple Regge couplings. The new low-mass, high-energy deuterium data[1] provide an additional constraint for the determination of these couplings. Our fit (12) was constrained to satisfy the new data via the FMSR, while that of Ref. 11 fails to do so by about 40%.

We wish to thank Dr. Vladimir Rittenberg for many useful discussions.

REFERENCES

1. Y. Akimov et al., Phys. Rev. Letters 35, 763 (1975).
2. Y. Akimov et al., Phys. Rev. Letters 35, 766 (1975).
3. See, for example, D.P. Roy and R.G. Roberts, Nucl. Physics B77, 240 (1974) and references therein.
4. A.I. Sanda, Phys. Rev. D6, 280 (1972); M.B. Einhorn, J. Ellis, and J. Finkelstein, Phys. Rev. D5, 2063 (1972).
5. Y. Akimov et al., Phys. Rev. D12, 3399 (1975).
6. A.S. Carroll et al., FERMILAB-Pub-75/51 -EXP.
7. V. Bartenev et al., Phys. Letters 51B, 299 (1974).
8. K. Abe et al., Phys. Rev. Letters 31, 1527 (1973).
9. M.G. Albrow et al., Nucl. Phys. B72, 376 (1974).
10. V. Bartenev et al., Phys. Rev. Letters 31, 1088 (1973).
11. R.D. Field and G.C. Fox, Nucl. Phys. B80, 367 (1974).

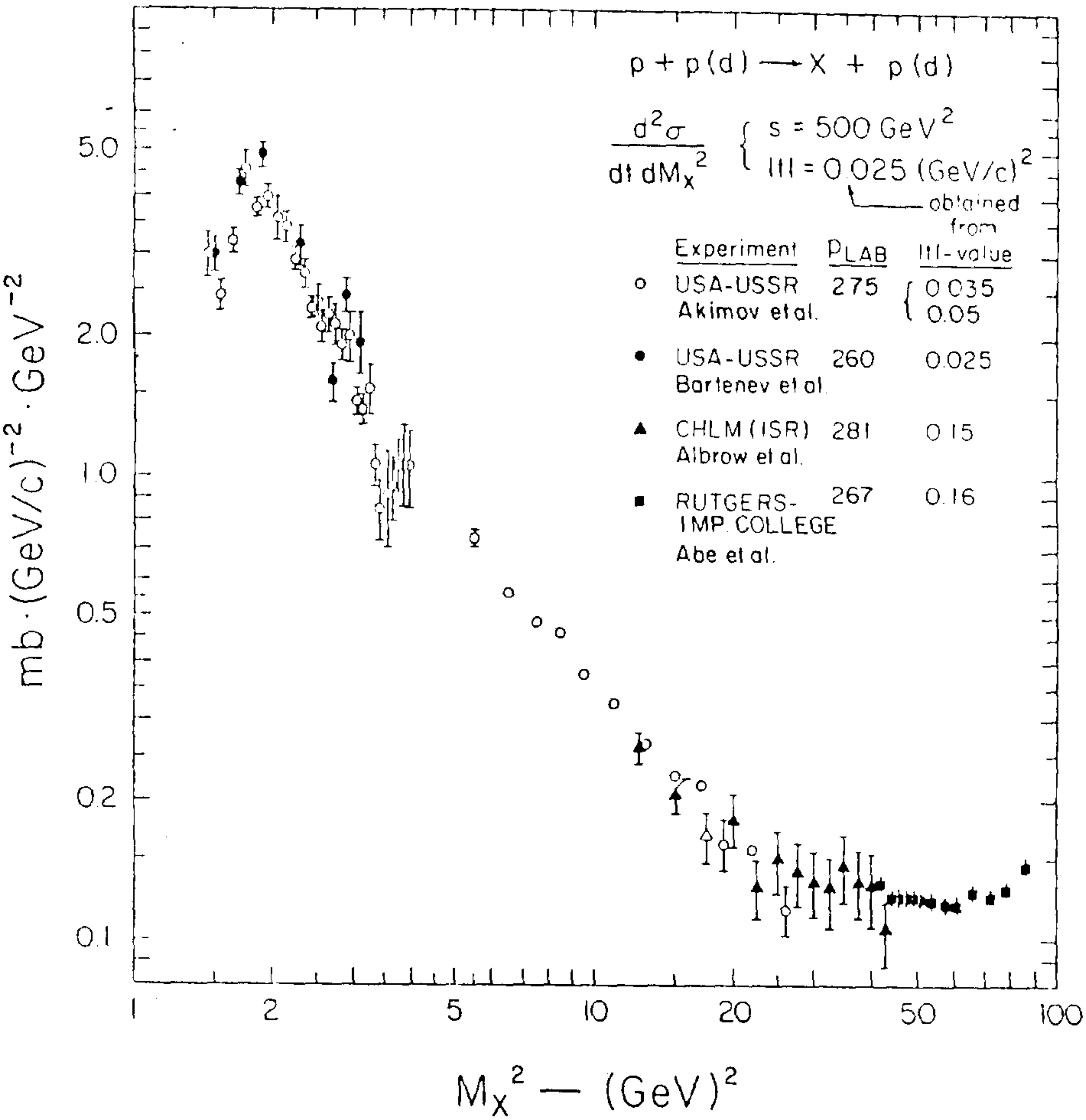

Figure 1 - Differential cross-sections for pp → Xp vs. M_X^2 for s ~ 500 GeV² and |t| = 0.025 (GeV/c)², obtained from the listed |t|-values using slopes given in the references. For the extrapolation of the CHLM and Rutgers — Imperial College data a slope of 6 $(GeV/c)^{-2}$ was used.

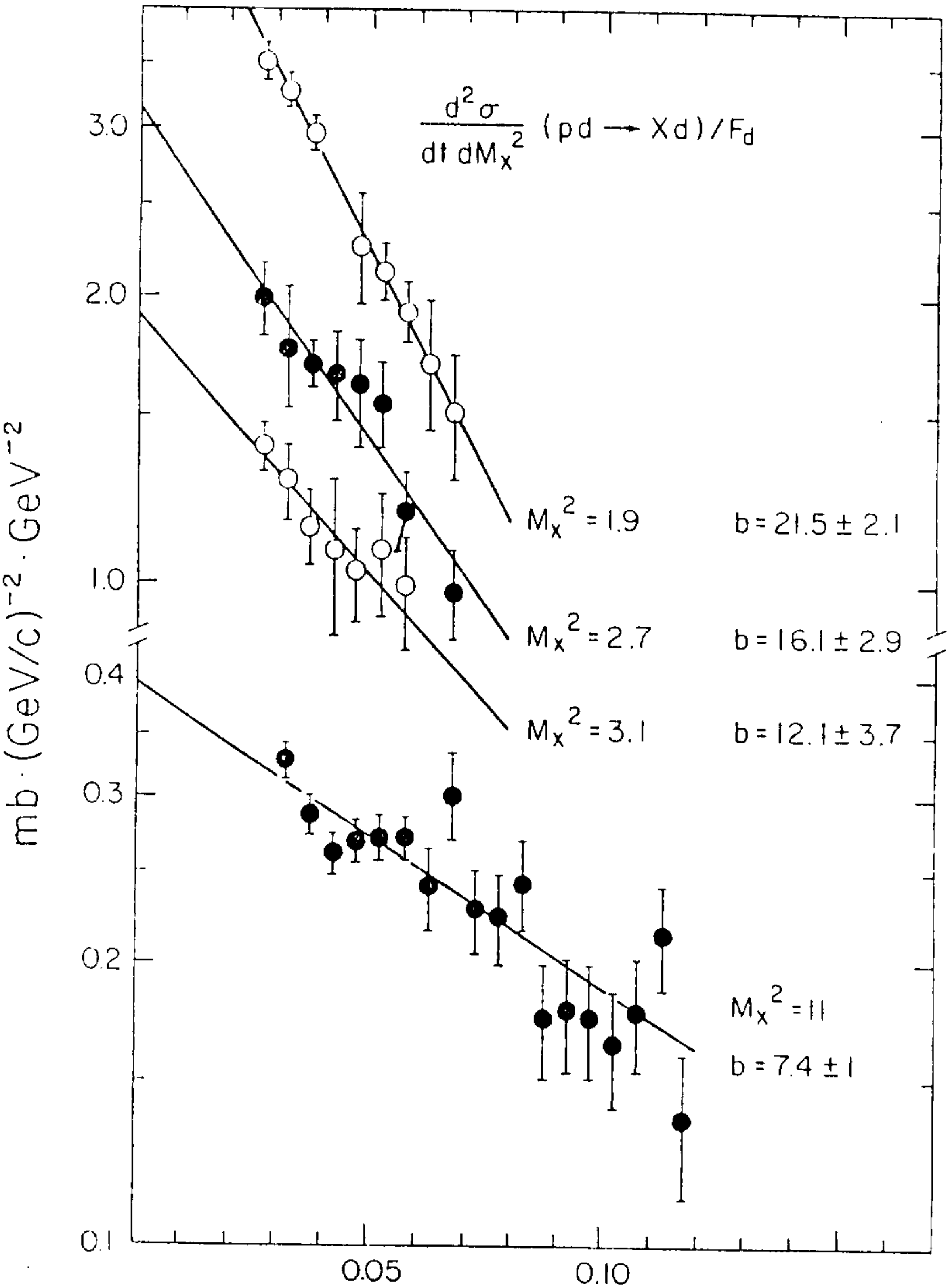

Figure 2 - Differential cross-sections vs. t for pp → Xp, extracted from pd → Xd, at p_{lab} = 275 GeV/c, for M_X^2 = 1.9, 2.7, 3.1, and 11 GeV^2.

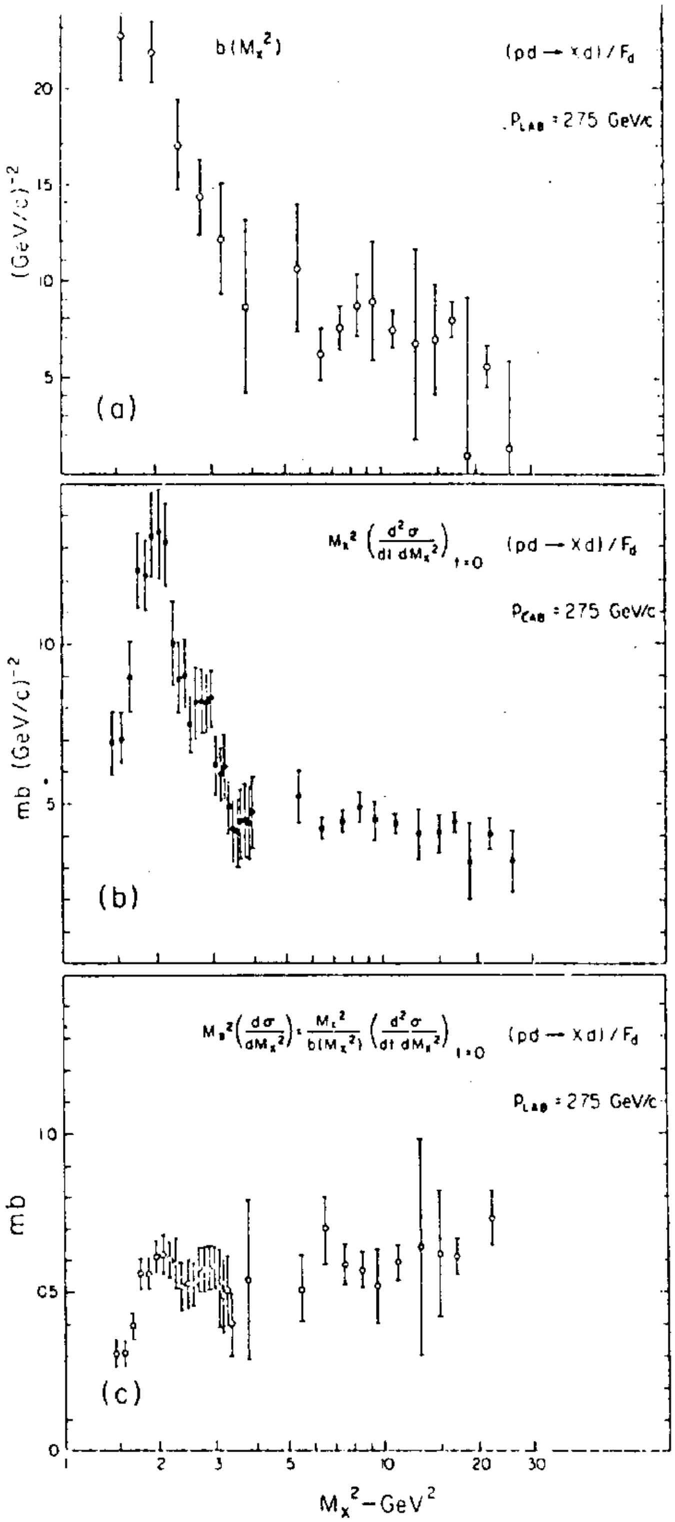

Figure 3 - Values for pp → Xp vs. M_X^2, extracted from pd → Xd at 275 GeV/c.

a) The slope parameter, b (m_X^2).

b) $d^2\sigma/dtdM_X^2$ multiplied by M_X^2 and extrapolated to t = 0 using b (M_X^2).

c) Values of (b) above, divided by values of (a): M_X^2 $(d\sigma/dM_X^2)$.

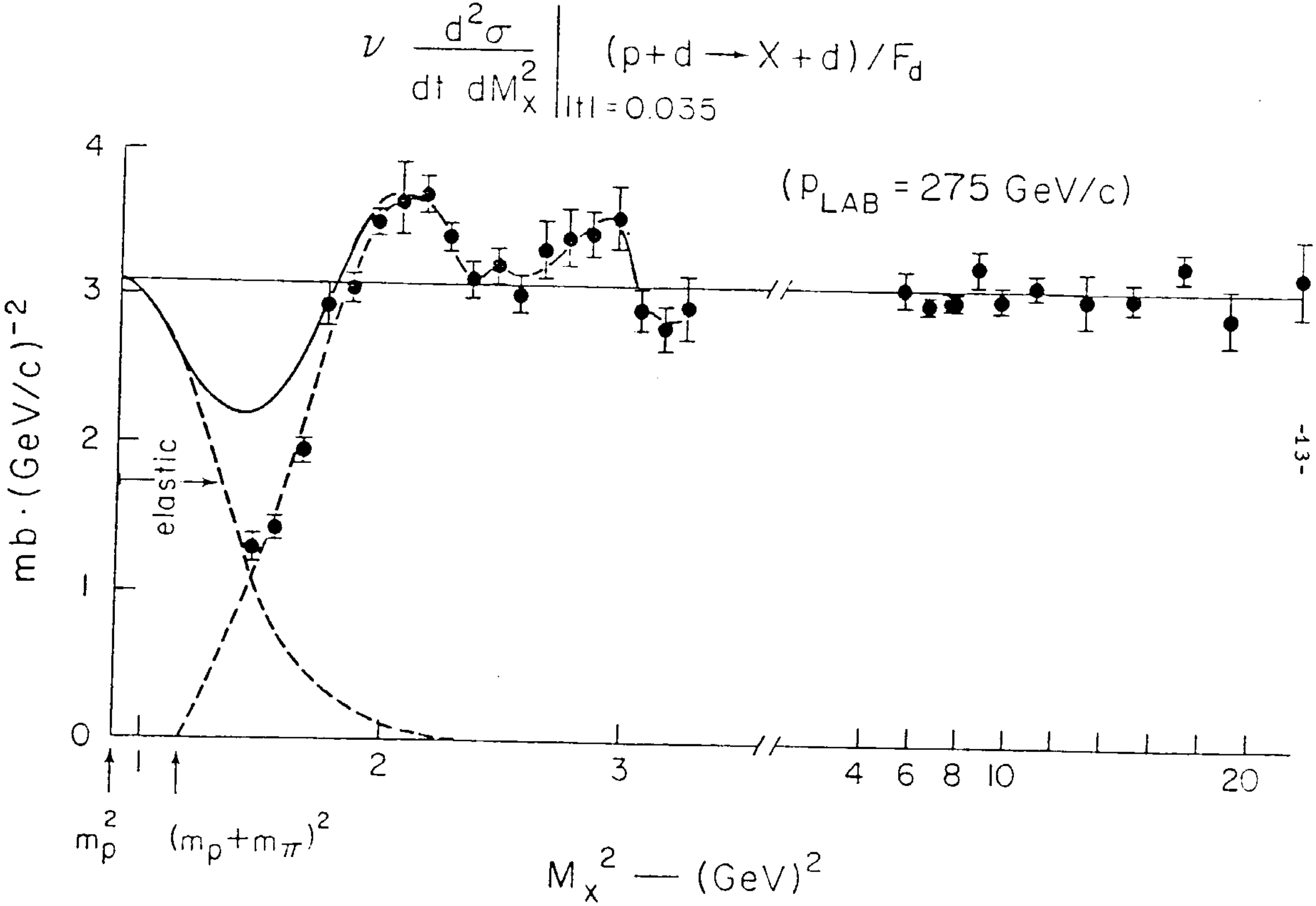

Figure 4 - Test of the first-moment FMSR: Values of $\nu(d^2\sigma/dtdM_x^2)$ vs. M_x^2 for p_{LAB} = 275 GeV/c and $|t|$ = 0.035 (GeV/c)^2